

Influence of Sedimentary Environment on the Structural Characteristics of Rock Layers Surrounding Roadways

Zhongsi Dou^{1,2}, Zhenghai Zhang¹ and Ruili Han^{3,*} and Yimeng Wang⁴

¹School of Civil and Architectural Engineering, East China University of Technology, Nanchang 330013, China

²Engineering Research Center for Digital Risk Control of Underground Engineering of Jiangxi Province, East China University of Technology, Nanchang, 330013, China

³School of Earth Sciences, East China University of Technology, Nanchang 330013, China

⁴School of Science and Engineering, University of Dundee, Dundee DD1 4HN, UK

Received 19 January 2025; Accepted 11 April 2025

Abstract

The deformation and failure of rocks surrounding roadways mainly depend on the strength and stress of the rocks. The strength of surrounding rocks is closely related to their structure. A reasonable study of the structural characteristics of rocks surrounding roadways is of great significance to the safe production of mines. To investigate the structural characteristics of roadway surrounding rock strata, this work selected the floor strata of the main mining coal seam of the Luling Mine in Huaibei, Anhui, China as the research subject. The lithology of the strata revealed by boreholes along major exploration lines and representative primary sedimentary structures in the study area was interpreted through sedimentary structure analysis. Subsequently, the thickness, properties, and structural features of various lithologies between No.8 coal seam floor and No.10 coal seam roof in the Luling Mine were systematically analyzed using data from 75 boreholes. The rock mass structure types in the study area were classified in accordance with the uniaxial compressive strength categorization of coal measure rock test specimens. Results demonstrate that: A delta system coal-bearing rock series dominated by river action is deposited in the Luling mining area. The total thickness of the main coal seam is 64.00~119.00 m, with an average of 82.32 m. Specifically, the thickness of sandstone is about 5.00~62.40 m, with an average of 33.77 m; the thickness of mudstone is about 19.80~91.00 m, with an average of 48.55 m; the sandstone content is 6.00%~75.00%, with an average of 41.00%; the mudstone content is 25.00%~94.00%, with an average of 59.00%. The coal seam floor is divided into two types of sedimentary rock layer structure, i.e., the whole mudstone type and the sand mudstone interbedded type. The whole mudstone type is interdistributary bay-crevasse splay model deposition, mud sand combination, which belongs to soft rock mass. The sand-mudstone interbedded type is a flooded basin-distributary channel model deposition, sand-mud combination, which belongs to medium-hard rock mass. Two engineering geological models of whole mudstone type and sand-mudstone interbedded type are established. The proposed study results provides foundational research data for analyzing the deformation mechanisms of roadways and their support.

Keywords: Sedimentary environment, Crevasse splay, Flood basin, Distributary channel

1. Introduction

The stability of rocks surrounding roadways is an important factor determining the safety of roadways. The deformation and failure of surrounding rocks mainly depend on their strength and the force acting on them. The strength of surrounding rocks is determined by their lithology, and the force of roadways depends on their buried depth and the geological structure. Coal seam mining during extraction significantly affects the stability of a floor roadway's surrounding rock, with mining-induced effects leading to increasingly prominent issues in roadway maintenance and rehabilitation [1-3].

The strength of surrounding rocks in roadways is influenced by multiple factors, including mining techniques, the size of the working face, and geological and structural conditions [4-6]. Since the middle of the 20th century, with the branch refinement of the development direction of rock

mechanics, important progress has been made in the study of the stability of the surrounding rock mass of roadways. The method has developed from the original elastic and elastic-plastic methods to rheology, damage, expansion, and fracture. With the rapid development of computer science and technology, auxiliary software has also emerged at the historic moment, providing a strong and effective guarantee for the study of the stability of the rock mass structure of roadways. Some researchers use various numerical simulation software to conduct theoretical analysis by adjusting parameters [7,8], while some adopt the method of setting up measurement points underground and utilize advanced monitoring technologies to collect and analyze data [9,10]. However, numerical simulation analysis cannot fully and objectively reflect the actual complex geological conditions underground, and underground measurement cannot be fully carried out because of the high cost required, which brings great technical problems to the study of the influence of the geological structure of rock layers on the deformation of roadways.

*E-mail address: 863797976@qq.com

ISSN: 1791-2377 © 2025 School of Science, DUTH. All rights reserved.

doi:10.25103/jestr.182.06

On this basis, this study investigated the environmental formation processes of sedimentary rock layers. The lithology and representative primary sedimentary structures of rock strata exposed by boreholes along key exploration lines in the study area were systematically interpreted. Sedimentary depositional patterns within the interval spanning from the base of No. 8 coal seam to the roof of No. 10 coal seam were thoroughly analyzed. Two distinct engineering geological models—full mudstone type and sand-mudstone interbedded type—were subsequently developed. This study provides foundational research data for analyzing the deformation mechanisms of roadways.

2. State of the art

For the study of sedimentary environment theory, Shea-Albin, Mark C, and other scholars first used sedimentary petrology theory to assess the stability of roadway surrounding rocks [11,12]. Lander R H adopted two 3D simulation methods to reflect sedimentary petrology and enrich the theory of sedimentary petrology [13].

Many studies have been performed on the influence of sedimentary environment theories on lithofacies structures. Milad Benmadi et al. conducted detailed lithofacies identification on the exposed outcrops of Wutong Rock in Mississippi, USA and the SCOOP underground wells in the central-southern part of Oklahoma, USA to study the sedimentary environment and lithofacies of Wutong Rock, and the results can be used for underground prediction to strengthen exploration and development plans [14]. P. Antipov et al. investigated the tectonic and sedimentary environments of the hydrocarbon-bearing Triassic sequences in the Caspian region, demonstrating that the area was dominated by marine terrigenous carbonate rocks, sedimentary rocks, and volcanoclastic deposits, while the structural characteristics of the Pre-Caspian Basin sequences exhibited a genetic relationship with salt tectonics [15]. Ramkumar M et al. conducted a study on basin-scale fluvial sediments in sedimentary environments, which contributed to the understanding of various lithologic structures of sediments [16].

Few studies exist on the surrounding rock strata of roadways from the perspective of sedimentary environment. Hylbert et al. analyzed the influence of river channel action and crevasse splay deposition on the stability of roadway roof [17]. Houseknecht evaluated the main geological factors affecting the stability of coal seam roof from the perspective of sedimentation [18]. Shear Albinv. R believed that the stability of coal seam roof is related to the sedimentation of coal seam surrounding rock, early compaction strength, late structural characteristics, and other factors [19]. Considering the sedimentary conditions of coal seam and its roof formation, Chinese scholars have established different regional sedimentary models to analyze the stability of coal seam roof. Chen Jiangfeng et al. applied methods such as sedimentary petrology and, building upon the AHP-fuzzy comprehensive evaluation model, utilized Mathematica to conduct a comprehensive zoning analysis of No. 4 coal seam roof in Huangyuchuan Coal Mine, Inner Mongolia, China, concluding that rock mechanical properties and structural development degree exerted significant control over roof stability [20]. Zhen et al. systematically analyzed the stability of the roof surrounding rock in an inclined coal seam and determined the key factors of surrounding rock deformation in different stages of GEF

support process [21]. Yuan Yue studied the problems of large deformation and failure of soft rock roadways in deep coal seam roofs and summarized the failure mechanism and control countermeasures for surrounding rocks of roadways in intercalated coal seams [22]. Chinese scholar Li Dezhong studied the equivalent elastic characteristics of sedimentary rock layers, where each rock layer in the stratified rock mass structure was treated as a homogeneous and isotropic elastic body, and proposed that the elastic characteristics of the equivalent medium could be represented by the stratified thickness and elastic constants of the sedimentary rock layers; this equivalent medium is capable of replacing multilayered, discontinuous rock masses within a certain range, thereby providing a simplified analytical method for studying the properties of sedimentary rock layers [23]. Abhishek Batwara et al. established a coal seam geological model of ultrafine Mannville Formation, revealed the rock properties of sedimentary coal seams, and improved the efficiency of coal seam mining [24]. Peng Jun et al. investigated the basic sedimentary characteristics and development models of fine-grained sedimentary rocks by studying the sedimentary structure and rock formation types of the Qianfoya Formation in the Yuanba area [25].

Scholars have conducted extensive research through analyses of sedimentary environments, lithology of rock masses, and stratigraphic combination structures of coal-bearing strata. However, their research focus remains primarily on evaluating the stability of coal mine roofs and floors on the basis of sedimentary rock layer structures. Stratigraphic characteristics and sedimentary models require further in-depth exploration from the perspective of depositional environments.

The rest of this study is organized as follows: Section 3 indicates the detailed analysis of the sedimentary environment of the main coal seam in the study area. Section 4 presents the interpretation of the lithology type and sedimentary model of the rock strata in the study area and the identification of the lithology structure characteristics of the main coal seam floor. Section 5 summarizes the results of this study and provides relevant conclusions.

3. Methodology

3.1 Sedimentary environment of the main coal seam section

To analyze the sedimentary environment of the main coal seam section of the Luling Mine, this study identified and interpreted the lithology and representative primary sedimentary structures revealed by the boreholes of the main exploration lines in the mining area. Based on the analysis of the sedimentary characteristics of the Permian coal-bearing rock series in the Huaibei Coalfield by Li Yunshan et al., the Luling Minefield belongs to the epicontinental sea environment in the Carboniferous period. From the early Permian period, the sea water gradually withdrew from north to south, the effect of the distributary channel was strengthened, and the delta prograded to the sea basin. A delta system coal-bearing rock series dominated by river action was deposited in this area [26,27].

The following diagram shows the primary sedimentary structure and biological sequence formed by the deltaic sedimentary environment in the study area, with the representative sedimentary structure name used to label the sedimentary unit formed by a certain role, and genetic explanation is given. The division of subenvironment and

microenvironment of the river-dominated delta system is shown in Table 1.

Table 1. Subenvironment and microenvironment division table of the delta system

Sedimentary Environment	Sub Environment	Microenvironment
river-dominated delta	delta-plain	distributary channel
		natural levee crevasse splay flood basin diversion Bay peat swamp
	delta front	estuary sandbar remote sand dam
	prodelta	

3.1.1 Delta plain

The delta plain is the water-based part of the delta, mainly influenced by river action, and is a vast and low-lying area.

(1) Distributary channel

The sediments of the distributary channel are generally medium-fine grained quartz sandstone, which transits upward to fine sandstone and mudstone. The sandstone has large and medium-sized cross bedding, and the bedding scale becomes smaller upward. There are retained sediments at the bottom, and the sorting is better.

Figure 1 depicts the sedimentary sequence of the upper part of the Lower Shihezi Formation in the 83-9 borehole of the minefield. The bottom of the sequence is No. 7 coal and mudstone roof, the lithology upward is medium-grained quartz sandstone, and trough cross-bedding is common. The upper sandstone is well-sorted fine-grained quartz sandstone,

which belongs to distributary channel deposition and often develops wedge-shaped cross-bedding. The upper part is natural levee sedimentary siltstone with slow wavy bedding and No. 6 peat swamp sedimentary coal. The sedimentary sequence in the upper part of the Shihezi Formation under the hole of 83-9 reflects the weakening of the hydrodynamic conditions of the distributary channel or the process of channel migration in the deposition.

(2) Natural levee

The natural levee deposit is often associated with the sedimentary facies of the distributary channel. The sedimentary lithology is mainly siltstone, with gentle wavy bedding and small sandy bedding. It is mainly formed by the deposition of suspended solids on the embankment during the flood period, as shown in Fig. 1.

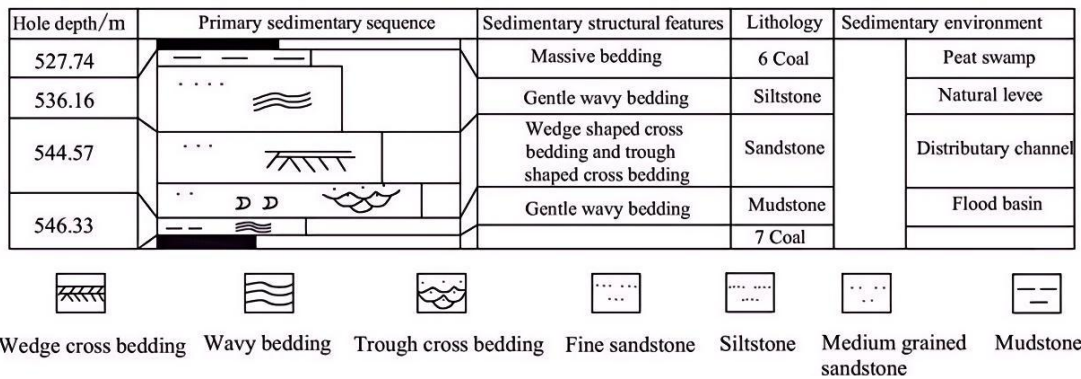


Fig. 1. Sedimentary sequence of upper part of the lower Shihezi Formation (hole 83-9)

(3) Crevasse splay

The crevasse splay is deposited because the estuary of the distributary channel is seriously blocked, and the water volume in the distributary channel continues to increase, causing the estuary to break the embankment. Then, the deposition is formed. Crevasse splay deposits often appear on the interdistributary bay or flood basin. The lithology of the sedimentary strata is mainly medium and fine-grained sandstone with poor roundness and sorting, and most of them form small cross-bedding with positive grain sequence, as shown in Fig. 2.

Fig. 2 depicts the sedimentary sequence of the lower part of the Lower Shihezi Formation in the minefield. The aluminous mudstone layer (K2) at the bottom belongs to the flood basin deposit. The upper sedimentary rock is medium-sorted quartz sandstone, which belongs to the crevasse splay deposit, with massive bedding. The upper part is the flood basin and peat swamp deposit mudstone and No. 9 coal.

(4) Flood basin

The area where the floodplain of the delta plain is deposited during the flood period is called the floodplain basin. The lithology of the sedimentary strata in the alluvial basin is mainly composed of siltstone and mudstone. Developed undulating laminations and horizontal laminations mainly exist, and common plant fossils are also found. The deposition of alluvial fans is more abundant than that of distributary channels and alluvial fans before and after the outburst, as shown in Figure 2.

(5) Peat swamp

It is commonly found in deltaic plain areas. With the continuous accumulation in the floodplain, the water depth becomes shallow. Then, with the extensive sea retreat in the region, the water body in the sedimentary basin gradually becomes shallow, and swampification progressively develops, forming peat swamps (Figure 2).

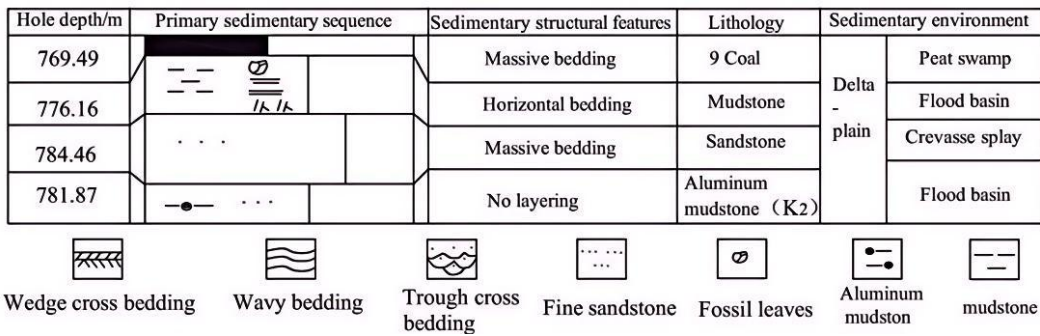


Fig. 2. Sedimentary sequence of lower part of the lower Shihezi Formation (hole 00-2)

(6) Interdistributary bay

The sedimentary lithology of the interdistributary bay is primarily gray-black mudstone, which is mainly formed in a relatively stable hydrodynamic environment. The interdistributary bay is easy to be silted up to form peat swamp, which provides favorable conditions for the deposition and formation of coal seams. Fig. 3 presents the sedimentary sequence of the middle part of the Lower Shihezi Formation in the Luling Minefield. The lower

section is mudstone deposited in the interdistributary bay environment, often with horizontal bedding structure; the sedimentary facies in the middle section are interdistributary bay facies and crevasse splay facies. The main lithology is fine sandstone with small thickness and thick mudstone, which reflects the weak hydrodynamic conditions of the water. The upper section is the mudstone deposition of the flood basin.

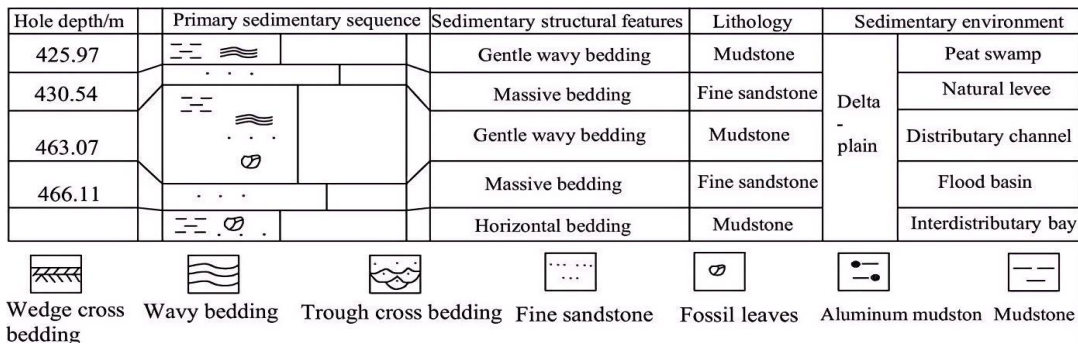


Fig. 3. Sedimentary sequence of the middle part of the lower Shihezi Formation (hole 00-1)

3.1.2 Delta front

The delta front is the area where the water from the river with sand content enters the basin and is the underwater part of the delta. At the confluence of the distributary river, owing to the sudden change in water dynamic conditions, the water energy decreases, causing the sediment to settle down.

(1) Estuary sandbar

The deposition of the estuary sandbar is due to the fact that the sand river water in the distributary channel enters the open water area of the basin, the water flow velocity decreases, and the sand body is deposited in large quantities. The estuary sand dam deposit is close to the distributary channel, and mudstone deposits such as interdistributary bay are common on it, as shown in Fig. 4.

(2) Remote sand dam

The distal sandbar deposits are located above the pretriangular plain deposits, as demonstrated in Figure 4. They belong to the same pretriangular plain deposits as the estuarine sandbar deposits. The sediment is mainly composed of interbedded sand and mud rocks, and common fossils of organisms and other features are also found.

3.1.3 Prodelta

The fore delta is the bottom fine-grained sequence of deltaic sedimentation, with horizontal bedding structure. The lithology is mostly dark mudstone, and it is located beneath the distal sandbar deposit, as shown in Figure 4.

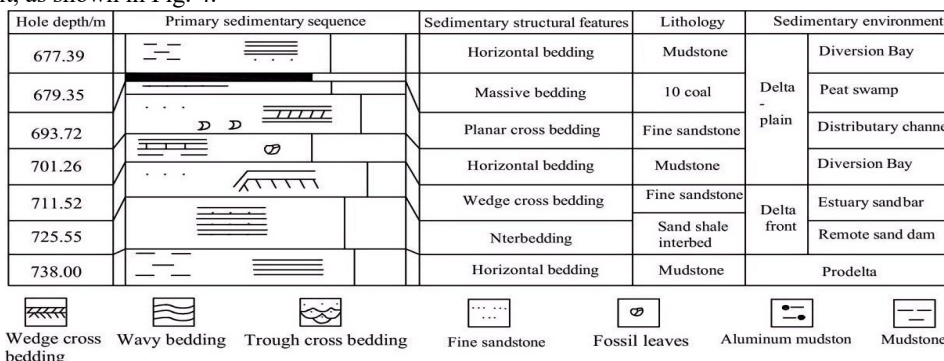


Fig. 4. Sedimentary sequence of the lower part of Shanxi formation (hole 92-3)

3.2 Primary sedimentary structure sequences and their environmental interpretation

The formation of primary sedimentary structures is strictly controlled by sedimentary environmental factors. Through the study of the constructive deltaic sedimentary environment and sedimentary structural characteristics

dominated by river action in the abovementioned research, the primary sedimentary structure sequence of the Permian coal series in this mining area and the corresponding sedimentary environment are summarized, as shown in Table 2. This information provides a basis for the analysis of the sedimentary facies of No. 8 coal seam floor.

Table 2. Primary tectonic sequence and interpretation of sedimentary environment in Luling mine

General Lithology	Representative Primary Sedimentary Structures	Sedimentary Environment	
coal	massive bedding	Peat swamp	delta-plain
Mudstone and siltstone	Horizontal bedding and gentle wavy bedding	flood basin	
sandstone	Block bedding and small cross bedding	crevasse splay	
siltstone	Slow wavy bedding and small ripple bedding	natural levee	
sandstone	Large and medium-sized cross bedding	distributary channel	delta front
Mudstone and siltstone	Horizontal bedding and wavy bedding	Diversion Bay	
sandstone	Wedge-shaped cross bedding	Estuary sandbar	
sand shale interbed	Interbedding	Remote sand dam	prodelta
mudstone	horizontal bedding		

4. Result Analysis and Discussion

The lithologic types and their degree of softness and hardness of coal measures have a significant effect on the stability of well engineering [28-30]. To determine the types of coal-bearing rock formations and their hardness and softness, this study classified the coal-bearing rocks into two major categories: mudstone type (carbonaceous shale, coal seam, mudstone, sandy mudstone, etc.) and sandstone type (fine sandstone, medium sandstone, coarse sandstone, and conglomerate). On the basis of the data from the previous exploration boreholes of the mine, the rock types of the strata between the bottom of No. 8 coal seam and the top of No. 10 coal seam were analyzed, obtaining the rock type composition characteristics of each stratum section.

4.1 Lithologic composition of the floor strata of the main coal seam

The composition of rocks in the rock stratum section from the bottom of No. 8 coal seam to the top of No. 10 coal seam in the Luling Mine was statistically analyzed, and the results are presented in Table 3. The total thickness of this section ranges from 64.00 m to 119.00 m, with an average of 82.32 m. In particular, the thickness of the sandstone layer is approximately 5.00~62.40 m, with an average of 33.77 m; the thickness of mudstone is approximately 19.80~91.00 m, with an average of 48.55 m; the content of sandstone-like rocks ranges from 6.00% to 75.00%, with an average of 41.00%; the content of mudstone types ranges from 25.00% to 94.00%, with an average of 59.00%. From this information, the strata from the bottom of No. 8 coal seam to the top of No. 10 coal seam in the Luling Coal Mine are mainly composed of mudstone.

Table 3. Lithology thickness from the floor section of No.8 coal seam to the top section of No.10 coal seam in Luling mine.

Hole number	sandstone thickness/m	Thickness of mudstone/m	Total thickness/m	Sandstone content/%	mudstone content/%	Hole number	sandstone thickness/m	Thickness of mudstone/m	Total thickness/m	Sandstone content/%	mudstone content/%
91-3	57.2	19.8	77.0	74.3	25.7	78-1	38.0	50.0	88.0	43.2	56.8
hole4	54.4	20.3	74.7	72.8	27.2	98-1	35.0	50.3	85.3	41.1	58.9
91-5	62.2	20.9	83.1	74.9	25.2	92-3	20.0	52.0	72.0	27.5	72.2
78-4	51.0	21.2	72.2	70.6	29.4	11-2	33.0	53.0	86.0	38.4	61.6
81-7	62.4	21.6	84.0	74.3	25.7	92-5	33.0	53.0	86.0	38.4	61.6
83-4	46.5	23.7	70.2	66.2	33.8	83-2	29.2	53.6	82.8	35.3	64.7
106	62.0	24.0	86.0	72.1	27.9	92-3	20.5	54.5	75.0	27.3	72.7
94-1	56.5	28.4	84.9	66.6	33.5	91-3	19.3	54.5	73.8	26.1	73.9
86-1	40.0	29.0	69.0	58.0	42.0	CQ-5	28.3	55.3	83.5	33.8	66.2
98-1	56.8	29.9	86.7	64.84	34.1	89-2	36.0	56.0	92.0	39.1	60.9
LU5	36.0	41.0	77.0	46.8	53.3	18-2	34.0	66.0	100.0	34.0	66.0
104	44.0	30.0	74.0	59.46	40.5	82	43.0	56.0	99.0	43.4	56.6
water2	55.0	31.0	86.0	64.0	36.1	94-4	30.0	56.0	86.0	34.9	65.1
81-9	46.9	31.1	78.0	60.1	39.9	90-4	31.0	56.0	87.0	35.6	64.4
14-2	55.3	33.0	88.3	62.6	37.4	91-4	13.8	56.3	70.0	19.6	80.4
12-3	55.0	33.0	88.0	62.5	37.5	LU1	27.0	57.0	84.0	32.1	67.7
138	56.0	33.0	89.0	63.6	37.5	94-7	17.0	57.0	74.0	23.0	77.0
170	56.0	34.0	90.0	62.2	37.8	92-4	24.0	57.0	81.0	29.6	70.4
19	49.0	34.0	83.0	59.0	41.0	92-8	30.0	57.0	87.0	34.5	65.5
28-2	42.0	35.0	77.0	54.6	45.5	94-5	18.0	58.0	76.00	23.7	76.3
12-2	50.0	35.0	85.0	58.8	41.2	81-15	23.4	58.6	82.0	28.5	71.5
78-3	47.0	35.0	82.0	57.3	42.7	137	33.0	59.0	92.0	35.9	64.1
13-3	32.1	35.2	67.3	47.7	52.3	92-1	23.0	60.0	83.0	27.7	72.3
94-3	36.2	35.8	72.0	50.3	49.7	95-1	24.0	60.0	84.0	28.6	71.4
81-1	44.0	36.0	80.0	55.0	45.0	92-2	17.0	61.0	78.0	21.8	78.2
83-11	31.0	37.0	68.0	45.6	54.4	91-4	12.0	61.0	73.0	16.4	83.6
79-20	50.0	37.0	87.0	57.5	42.5	133	15.0	62.0	77.0	19.5	80.5
9-102	44.0	38.0	82.0	53.7	46.3	94-1	17.0	63.0	80.0	21.3	78.8
83-13	32.0	40.0	72.0	44.4	55.6	83-12	37.0	64.0	101.0	36.6	63.4
78-2	42.0	40.0	82.0	51.2	48.8	98-2	38.0	65.0	103.0	36.9	63.1
83-3	37.1	40.0	77.1	48.1	51.9	91-1	9.0	65.0	74.0	12.2	87.8
83-9	33.0	42.0	75.0	44.0	56.0	83-10	22.8	67.3	90.0	25.3	74.7
73-3	19.0	45.0	64.0	29.7	70.3	89-1	13.0	68.0	81.0	16.1	83.4
6-7-9	24.0	45.8	69.8	34.4	65.6	190	12.0	71.0	83.0	14.5	85.5
28-10	29.1	45.9	75.0	38.8	61.2	93-1	7.4	71.9	79.3	9.3	90.7

83-14	25.0	46.0	71.0	35.2	64.8	94-6	41.0	72.0	113.0	36.3	63.7
91	34.0	46.0	80.0	42.5	57.5	98-2	26.3	73.5	99.8	26.3	73.7
28-9	28.2	46.8	75.0	37.6	62.4	83-10	15.0	77.0	92.0	16.3	83.7
81-16	32.3	46.9	79.2	40.8	59.2	81-14	27.0	80.0	107.0	25.2	74.8
98-3	25.0	47.0	72.0	34.7	65.3	81-13	5.0	80.0	85.0	5.9	94.1
97	33.0	48.0	81.0	40.7	59.3	183	28.0	91.0	119.0	23.5	76.5
83-9	24.75	49.0	73.8	33.6	66.4						

4.2 Lithologic combination characteristics of the floor strata of the main coal seam

Based on the statistical analysis of the data from 75 boreholes in the Luling coalfield that expose the section from the bottom of No. 8 coal seam to the top of No. 10 coal seam, two main types of combinations are developed within the coalfield. One is dominated by mudstone with thin layers

of sandstone or entirely composed of mudstone (the full mudstone type combination). The other is dominated by sandstone with mudstone or sand-mudstone interbedded layers (the sand-mudstone interbedded type combination). A comparison of their stratigraphic columns is shown in Figure 5.

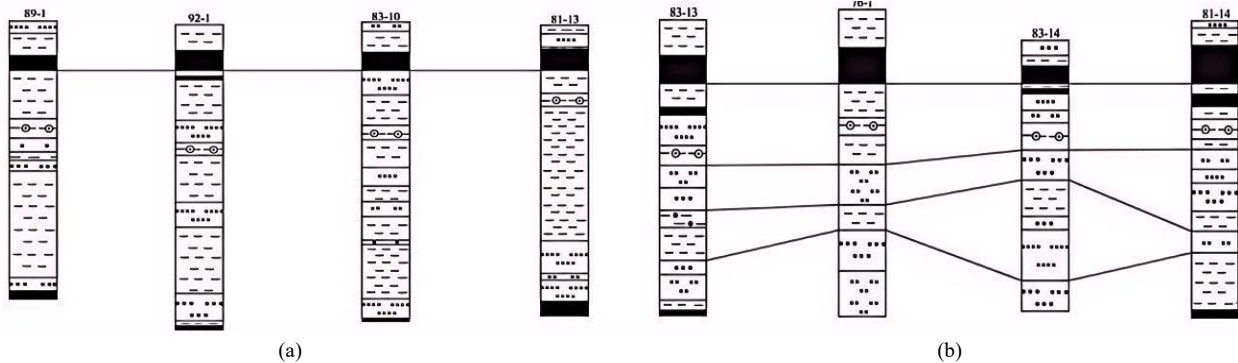


Fig. 5. Lithological association type of floor strata of No.8 coal seam in Luling mine. (a)All mudstone type combination. (b)Sand-mudstone interbedded type combination

4.3 Sedimentary mode of floor strata in the main coal seam

On the basis of the sedimentary background of the coal-bearing strata in this area, combined with the lithologic combination characteristics of No. 8 coal seam floor, and in accordance with the sedimentary facies indicators such as

lithology, biologic fossils, and bedding exposed by the boreholes, the main sedimentary patterns of No. 8 coal seam floor in this area were comprehensively determined to be two type: interdistributary bay-crevasse splay type and flooded basin-distributary channel type (Table 4).

Table 4. Classification of sedimentary models of No.8 coal seam floor in Luling mine

Type	Depositional Model	Lithological Composition	Rock Strength Grade	Expose Drilling Holes
I	Interdistributary bay-crevasse splay type	Mudstone as the main component, interbedded with fine sandstone	weak	89-1,92-1, 83-10,81-13
II	Flooded basin-distributary channel type	Medium sandstone, siltstone, fine sandstone	strong	83-13,83-14,76-1

4.3.1 Interdistributary bay-crevasse splay sedimentary model

The top of No. 10 coal is composed of gray-white fine sandstone with developed bedding, which is a distributary channel deposit. On the top is mainly dark gray and gray-black mudstone, containing a small amount of plant fossil fragments and siderite ooids, with the characteristics of horizontal bedding interdistributary bay sediments. At that time, the hydrodynamic conditions in the sedimentary basin of this area were weak, and the supply of terrigenous debris was minimal. The middle and lower part of No. 8 coal is an aluminous mudstone layer, with a small amount of siltstone, horizontal bedding, and plant root and leave fossils. This layer has stable development of aluminous mudstone, which is the boundary marker layer (K2) between the Lower Shihezi Formation and the underlying Shanxi Formation in the Luling Minefield, belonging to the flood basin deposit, and between the Lower Shizhibu Formation and the underlying Xiashan Formation in the Luliang Coalfield, belonging to the alluvial basin sedimentary environment. Above K2 is a layer of fine-grained quartz sandstone. The roundness and sorting of the particles are poor. Most of them

are massive bedding, with inconspicuous normal grain sequence crevasse splay deposits. On it is a set of flood basin and peat swamp deposits. The sediments of the flood basin are mainly mudstone and siltstone with horizontal bedding or slow wavy bedding. The peat swamp environment provides conditions for coal development.

4.3.2 Flooded basin-distributary channel sedimentary model

A layer of medium sandstone with a thickness of about 15 m exists at the top of No. 10 coal seam. It develops plate-like cross-bedding and often contains argillaceous inclusions. It belongs to the distributary channel deposit. Above it is the interdistributary bay deposit, mainly mudstone and sandy mudstone, and is sandstone and the distributary channel deposit with a thickness of 11 m. The aluminous mudstone in the middle and lower part of No. 8 coal is the flood basin deposit, and a peat swamp is developed on it. The peat swamp environment provides conditions for coal development.

4.4 Sedimentary rock structure type of the main coal seam floor

4.4.1 Rock lithology type of the main coal seam floor

On the basis of the uniaxial compressive strength of coal-bearing rock specimens, the rocks were classified into three types: hard, medium-hard, and soft rocks. For the coal-bearing rock formations, the percentage of hard rocks (K) was used to represent the characteristics of rock types:

$$K = \frac{h}{H} \times 100\% \tag{1}$$

where *h* represents the total thickness of medium-hard rock in a certain coal-bearing stratum section, and *H* represents the total thickness of the statistical stratum section. In accordance with the value of *K*, the types of rock mass were classified into three categories, namely, hard, medium-hard, and soft rock mass, as shown in Table 5. Under the influence of mining, different floor lithology types will produce varying stress transfer laws, which will also have a control effect on the deformation characteristics of the floor roadway in the stope.

Table 5. Rock mass type of coal seam floor

Lithological type of bottom rock mass	K value (%)	Main lithology
Hard rock mass	≥65	Various sandstones and limestone
Medium hard rock mass	35~65	Sandstone, silty mudstone, and mudstone
Soft rock mass	≤35	Mudstone, silty mudstone, and coal seams

On the basis of the statistical data of boreholes in the Luling Mine, a distribution map of rock types in the strata from the bottom of No. 8 coal seam to the top of No. 10 coal seam was compiled, as shown in Figure 6. This section is mainly composed of medium-hard and soft rocks, with minimal hard rock. The soft rock masses are mainly distributed in the mining areas such as 6, 7, II4, II6, III1, III4; the medium-hard rock masses are largely distributed in the mining areas such as 1, 2, 3, 4, 5, 8, III1, II2, II3, II8, and III8.

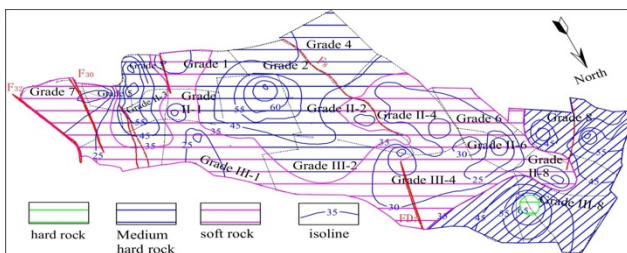


Fig. 6. Distribution pattern of rock types from the floor section of No.8 coal seam to the top section of No.10 coal seam in Luling Mine(The data in the figure for the sand rate /%)

4.4.2 Sedimentary rock structure type of the main coal seam floor

Controlled by the sedimentary environment, the sedimentary rock properties of coal measure stratum change cyclically in the vertical direction, forming different layered rock structures. According to the above comprehensive analysis of the lithology composition and its combination characteristics, sedimentary characteristics, and sedimentary model and lithology type of No. 8 coal seam floor, the coal

seam floor in this area can be divided into two types of sedimentary rock layer structure, namely, full mudstone type and sand mudstone interbedded type. The whole mudstone type is interdistributary bay-crevasse splay model deposition, mud sand combination, which belongs to soft rock mass. The sand-mudstone interbedded type is flooded basin-distributary channel model deposition, sand and mud combination, which belongs to medium-hard rock mass. The different sedimentary rock layer structures of the coal seam floor will affect the stress evolution of the stope floor and the deformation of the surrounding rocks of roadways.

5. Conclusions

To assess the structural characteristics of roadway surrounding rocks, this study interpreted the sedimentary environment and primary sedimentary structure sequence in the study area. Mine drilling data were used to analyze the lithologic composition, structural characteristics, sedimentary mode, and lithologic structure type of the main coal seam floor in the mine. The major conclusions are as follows:

(1) Based on the analysis of the sedimentary characteristics of the main coal seam in the Luling Mine, the main coal seam comprises a river-controlled deltaic sedimentary environment. The primary sedimentary tectonic sequence of the coal measures and the sedimentary environment represented by it were summarized. The sedimentary environment of No. 8 coal seam floor was determined to be dominated by the delta plain.

(2) The rock composition of No. 8 coal floor in the Luling Mine was statistically analyzed, from which mudstone rock accounts for the main part, followed by sandstone. Lithologic combination types of No. 8 coal seam floor in the mine were divided into full mudstone and sand-mudstone interbed.

(3) On the basis of the sedimentary environment of coal strata and the lithologic characteristics of No. 8 coal floor, combined with the data of biological fossils, two sedimentary models of interdistributary bay-crevasse splay type and flooded basin-distributary channel type were proposed. Combined with the lithology type, the engineering geological model of two kinds of sedimentary rock structure floors of full mudstone type and sand mudstone interbedded type was established. It provides a basis for studying the stress evolution of floor stope and the deformation and failure mechanism of floor roadways.

This study combines mine drilling data with sedimentology theory. On the premise that scientific, reasonable, and correct drilling sampling is ensured, it saves the research cost for roadway surrounding rock properties. It is suitable for mines with complete drilling data and has important practical significance. Owing to the specificity of the sedimentary model in the study area, partial generalization is inevitable. Therefore, in the analysis of surrounding rock strength and ground stress of a specific roadway, certain measurements should be combined to ensure accuracy and provide reasonable theoretical basis for support.

Acknowledgements

The authors are grateful for the support provided by the Doctoral research startup fund project of East China University of Technology (No. DHBK2019011) and Open Fund from Engineering Research Center for Digital Risk



References

- [1] A. Batugin, Z. Q. Wang, Z. H. Su, and S. S. Sidikovna, "Combined support mechanism of rock bolts and anchor cables for adjacent roadways in the external staggered split-level panel layout," *Int. J. Coal Sci Techn.*, vol. 8, no. 4, pp. 659-673, Jan. 2021.
- [2] W. W. Fang *et al.*, "Study on failure mechanism and control of surrounding rock of inclined strata crossing roadway in deep coal mine," *Front. Earth Sci.* to be published. Accessed: Jan. 16, 2024. doi: 10.3389/feart.2024.1338670. [Online]. Available: <https://doi.org/10.3389/feart.2024.1338670>
- [3] H. P. Ma, N. N. N. Daud, Z. M. Yusof, W. Z. Yaacob, and H. J. He, "Stability analysis of surrounding rock of an underground cavern group and excavation scheme optimization: Based on an optimized DDARF method," *Appl. Sci.*, vol. 13, no. 4, Feb. 2023, Art. no. 2152.
- [4] Z. H. Dong, X. Xi, Q. F. Guo, and Z. L. Feng, "Study on mining depth-strength response surface model of surrounding rock in fractured roadway," *Huazhong Keji Daxue Xuebao (Ziran Kexue Ban)/J. Huazhong Univ. Sci. Technol. (Nat. Sci. Ed.)*, vol. 50, no. 5, pp. 89-94, May. 2022.
- [5] C. X. Zhao, Y. M. Li, G. Liu, and S. J. Huang, "Study on surrounding rock support technology of deep soft rock roadway," *Meitan Kexue Jishu/Coal Sci. Technol.*, vol. 50, no. 4, pp. 76-84, Apr. 2022.
- [6] X. X. Yang, Y. Wu, and H. W. Jing, "Crack propagation and strength evolution law of roadway surrounding rocks based on in-situ ultrasonic tests," *J. Mining Saf. Eng.*, vol. 38, no. 3, pp. 528-537, Mar. 2021.
- [7] Z. Nurbek, K. Elvira, D. Vladimir, B. Anna, A. Rabbel, and S. Saule, "Ensuring a safe geomechanical state of the rock mass surrounding the mine workings in the Karaganda coal basin, Kazakhstan," *Min. miner. depos.*, vol. 17, no. 1, pp. 74-83, Mar. 2023.
- [8] P. Małkowski, Z. Niedbalski, and T. Balarabe, "A statistical analysis of geomechanical data and its effect on rock mass numerical modeling: a case study," *Int. J. Coal Sci Techn.*, vol. 8, no. 2, pp. 312-323, Oct. 2020.
- [9] O. Slashchova, O. Kohtieva, S. Rahimov, and V. Kharchenko, "Forecasting the risks of underground roadway stability loss based on mine research data," presented at the Proc. Int. Conf. Essays Min. Sci. Pract., Kiev, Ukraine, Jun. 18-20, 2024, Paper 012057.
- [10] J. D. Fernandez-Gutierrez, S. S. Rodriguez, H. Gonzalo-Orden, and H. Perez-Acebo, "Analysis of rock mass classifications for safer infrastructures," in Proc. XIV Conf. on Transp. Eng., Burgos, Spain, Jul. 6-8, 2021, pp. 606-613.
- [11] V. R. Shea-Albin, "Geological features that contribute to ground control problems in underground coal mines," *Inf. Circ.-U.S. Bur. Mines.*, Vol. 9370, Dec. 1993, Art. no. 160254.
- [12] C. Mark and G. M. Molinda, "The Coal Mine Roof Rating (CMRR) - a decade of experience," *Int. J. Coal Geol.*, vol. 64, no. 1-2, pp. 85-103, Oct. 2005.
- [13] R. H. Lander, J. E. Cook, J. Guilkey, A. Kerimov, L. M. Bonnell, and L. B. Goodwin, "Digital rock advances from a material point method approach for simulation of frame moduli and a sedimentary petrology-inspired method for creation of synthetic samples through simulation of deposition and diagenesis," *Geophysics.*, vol. 89, no. 1, pp. MR11-MR31, Jan. 2024.
- [14] M. Benmadi, S. Roger, and F. G. Zou, "Lithology, stratigraphy, chemostratigraphy, and depositional environment of the Mississippian Sycamore rock in the SCOOP and STACK area, Oklahoma, USA: Field, lab, and machine learning studies on outcrops and subsurface wells," *Mar. Petrol. Geol.*, Vol. 115, May. 2020, Art. no. 104278.
- [15] M. P. Antipov, V. A. Bykadorov, Y. A. Volozh, I. S. Patina, V. V. Fomina, and F. M. Bars, "Triassic Deposits in the Caspian Region: Structure, Tectonic Settings, Sedimentary Environments, and Oil-and-Gas Potential," *Lithol. Miner. Resour.*, vol. 59, no. 6, pp. 638-659, Nov. 2024.
- [16] M. Ramkumar *et al.*, "Textural characteristics of channel bed sediments and heavy minerals of the Cauvery River, Southern India: implications on depositional environments, provenance, tectonics and climate," *J. Sediment. Environ.*, vol. 10, no. 1, pp. 235-260, Feb. 2025.
- [17] D. K. Hylbert, "Developing geological structural criteria for predicting unstable mine roof rocks. Final contract report," *Int. J. Rock Mech. Min. Sci. Geomech. Abstr.*, vol. 16, no. 3, pp. 57, May. 1979.
- [18] D. W. Houseknecht and J. A. Kacena, "Tectonic and sedimentary evolution of the Arkoma foreland basin," *SEPM Midcontinent Sect. Guideb.*, vol. 1, pp. 3-33, Oct. 1983.
- [19] V. R. Shea-Albin, "Geological features that contribute to ground control problems in underground coal mines," *Inf. Circ.-U.S. Bur. Mines.*, Vol. 9370, Dec. 1993, Art. no. 160254.
- [20] J. F. Chen, H. T. Wu, J. B. Dong, C. P. Wang, and H. Dou, "Stability assessment of No.4 coal seam's roof in Huangyuchuan coal mine of inner Mongolia," *Chin. J. Geol. Hazard Control.*, vol. 27, no. 1, pp. 141-146, Feb. 2016.
- [21] E. Z. Zhen, S. Z. Dong, X. W. Xu, Y. J. Wang, and M. X. Wang, "Stability analysis and control countermeasures of surrounding rock of gob-side entry formed by roof-cutting in inclined coal seams," *Energy Explor. Exploit.*, vol. 42, no. 3, pp. 929-958, May. 2024.
- [22] Y. Yuan, F. B. Zhang, X. Shang, Z. Q. Liu, and G. Peng, "Deformation and failure analysis and control of deep roadway with intercalated coal seam in roof," *Chin. Saf. Sci. J.*, vol. 34, no. 1, pp. 158-165, Jan. 2024.
- [23] D. Z. Li, X. G. Xia, and C. Li, "Study on equivalent elastic feature of sedimentary formation in collieries," *Chin. J. Rock Mech. Eng.*, vol. 24, no. 18, pp. 3322-3326, Sep. 2005.
- [24] A. Batwara, J. Y. Wang, and I. D. Gates, "Ultraprecise model of a coal bed methane reservoir: Connectivity and implications for production," *J. Petrol. Sci. Eng.*, Vol. 217, Aug. 2022, Art. no. 110901.
- [25] J. Peng, X. Y. Zhang, T. Y. Xu, L. X. Cheng, K. Zhang, and B. Li, "Lithofacies characteristics and reservoir capacity of fine-grained sedimentary rocks of second member of Qianfoya Formation in Yuanba area, Sichuan Basin," *Petrol. Geol. Exp.*, vol. 46, no. 2, pp. 247-262, Mar. 2024.
- [26] Y. S. Li and E. L. Wei, "Sequence of primary sedimentary structures and sedimentary environment for the permian coal measures in the luling mine of the huaibei coal field," *Geol. Anhui.*, vol. 12, no. 1, pp. 29-34, Mar. 2002.
- [27] W. J. Wu, W. Z. Liu, and K. Q. Chen, "Analysis of sedimentary environments of permian strata in huaibei coal field," *Geol. Beijing.*, no. 3, pp. 21-25, Sep. 2000.
- [28] X. Z. Zhao *et al.*, "Geo-dynamic conditions instability and support optimization of semi coal-rock roadway in large inclined and extra thick coal seam," *Meitan Kexue Jishu/Coal Sci. Technol.*, vol. 50, no. 11, pp. 20-29, Nov. 2022.
- [29] Z. Y. Sun, Y. Z. Wu, Z. G. Lu, Y. L. Feng, X. W. Chu, and K. Yi, "Stability Analysis and Derived Control Measures for Rock Surrounding a Roadway in a Lower Coal Seam under Concentrated Stress of a Coal Pillar," *Shock Vib.*, vol. 2020, no. 1, pp. 1-12, Dec. 2020.
- [30] H. S. Jia *et al.*, "Failure law and classification control of extremely soft roof in mining roadway of unstable thickness coal seam," *Chin. J. Rock Mech. Eng.*, vol. 41, no. S2, pp. 3306-3316, Sep. 2022.